Tribological Journal BULTRIB Vol. 5, 2015
Papers from the International Conference **BULTRIB '15**
September 11-13, 2015, Sozopol, Bulgaria
Society of Bulgarian Tribologists
FIT – Technical University of Sofia

TRIBOLOGY OF METAL MATRIX MICRO- AND NANOCOMPOSITES

Aleksandar VENCL, Ilija BOBIĆ, Mara KANDEVA, Dimitar KARASTOYANOV

Abstract: *This paper presents a short summary of the researches conducted in past few years concerning the metal matrix composites with different matrix material, different reinforcing/alloying elements, and obtained by different processing techniques. The results are classified into three groups according to the matrix material. In the first group are the results for microcomposites with AlSi7Mg matrix alloy obtained by compocasting method. These results cover the influences of amount and size of reinforcement (Al_2O_3), and the influence of type of reinforcement (Al_2O_3, SiC and SiC with graphite addition). In the second group are the results for nanocomposites with ZnAl25Si matrix alloy obtained by casting and compocasting method. These results cover the influences of silicon and strontium addition percentage, and the influences of strontium and/or Al_2O_3 nanoparticles addition. In the third group are the results for micro- and nanocomposites with Cu matrix obtained by powder metallurgy technology (preceded by mechanical alloying and/or internal oxidation). These results cover the influence of size of reinforcement (Al_2O_3) on the macroscale (composite properties), and the same influence on the nanoscale (only the matrix properties).*

Key Words: *composite, A356 alloy, ZA-27 alloy, Cu powder, micro- and nano-sized Al_2O_3 particles, SiC and graphite particles, strontium.*

1. INTRODUCTION

The particulate composites with the aluminium-silicon (Al-Si) alloy matrix are one of the most commonly investigated metal matrix materials. Aluminium base provide these materials low density, good mechanical characteristics and high ductility, as well as excellent casting characteristics and high corrosion resistance. On the other hand, the reinforcements (mainly ceramic) improve the wear resistance of the matrix and the improvers (mainly graphite) reduce the coefficient of friction. The A356 Al-Si alloy (AlSi7Mg) is a casting alloy consisting of aluminium, silicon and magnesium and belongs to a group of hypoeutectic Al-Si alloys. This alloy has been widely applied in the machinery, aircraft and defence industries and particularly in the automotive industry [1].

The zinc-aluminium alloys are well-established zinc alloys with high aluminium content (8 to 28 wt. %). The alloy with 25 to 27 wt. % Al (ZA-27 alloy) is, due to the high strength and good wear resistance, frequently used for making sliding bearings intended for high load/low speed applications [2]. The dimensional stability over a period of time of ZA-27 alloy could be improved by replacing copper in the alloy with silicon (Zn-Al-Si alloys) [3]. By suitable additions of strontium to the Zn-Al-Si alloy (ZnAl25Si) the size of silicon particles can be reduced with its more uniform distribution [4]. The addition of the ceramic nanoparticles to the ZnAl25Si matrix alloy should have the similar role as the strontium addition.

The copper-based composites are used primarily for their excellent electrical and thermal properties, and reinforcements are added for control of thermal expansion or improved wear resistance. The matrix is usually the pure element to retain the excellent thermal or electrical properties [5]. In case when the reinforcement are the non-metallic particles, such as Al_2O_3, added to or formed within the copper matrix, the effectiveness of these oxide particles as strengtheners depends upon particle size (finer is better), particle distribution (well dispersed is better), particle density (more per unit volume is better), and particle spacing (closer is better) [6]. Applying the nanoscale tribological tests, by using an atomic force microscope, to the small and localized area (approx. few μm in diameter), it is possible to distinguish the influence that particles have on wear of the matrix (only the matrix properties) [7].

2. MATERIALS AND TRIBOLOGICAL TEST PROCEDURES

2.1. Microcomposites with AlSi7Mg matrix alloy (group I)

The matrix material was A356 hypoeutectic Al-Si alloy (EN AlSi7Mg0.3) with the following chemical composition (in wt. %): Al-7.2Si-0.02Cu-0.29Mg-0.01Mn-0.18Fe-0.01Zn-0.02Ni-0.11Ti. Composites were produced by applying the compocasting method, where the second phase particles were added into the semi-solid A356 alloy by infiltration and admixing. Experimental procedure and apparatus used for the compocasting processing are described and discussed elsewhere [8].

Composite specimens (Table 1) were subjected to heat treatment with following parameters: solution annealing at 540 °C for 6 h, water quenching and artificial aging at 160 °C for 6 h. The chemical composition of gray cast iron, chosen as the reference material, fabricated using the sand casting procedure followed with heating at 550 °C, was: Fe-3.18C-2.17Si-0.60Mn-0.7P-0.37Cr.

Table 1. Designation and properties of the tested materials (group I)

Specimen designation	Composition	Particle content, wt. %	Particle size, μm
A0	Gray cast iron (reference material)	–	–
A1	A356 + Al_2O_3	3	12
A2	A356 + Al_2O_3	10	12
A3	A356 + Al_2O_3	10	35
A4	A356 + SiC	10	39
A5	A356 + SiC + Gr (graphite)	10 (SiC); 1 (Gr)	39 (SiC); 35 (Gr)

Microstructures of the tested materials have been presented and discussed elsewhere [1, 8], as well as, the hardness and other mechanical properties [1, 9-12].

Tribological test were conducted in two phases: In the first phase (specimens A0, A1, A2 and A3) influences of amount and size of reinforcement were investigated, and in the second phase (specimens A3, A4 and A5) influences of type of reinforcement and graphite were investigated. Both tests were under dry sliding conditions, in ambient air at room temperature. The phase I tests were carried out on the standard pin-on-disc tribometer with cylindrical pins made of tested materials. Test parameters were as follows: sliding speed: 1 m/s; normal load: 1, 2, 3 and 4 MPa; sliding distance: 5000 m; counter-body: disc (nodular gray cast iron). The phase II tests were carried out on the ball-on-barrel tribometer with linear (reciprocating) movement. Moving body with cylindrical geometry was made of tested materials. Test parameters were as follows: sliding speed: 0.038 m/s (average); normal load: 1 N; sliding distance: 500 m; counter-body: ball (alumina). The values of coefficient of friction were monitored during both tests. Diagrams of the load, sample, counter body and the direction of movement for both tribometers are shown in Fig. 1.

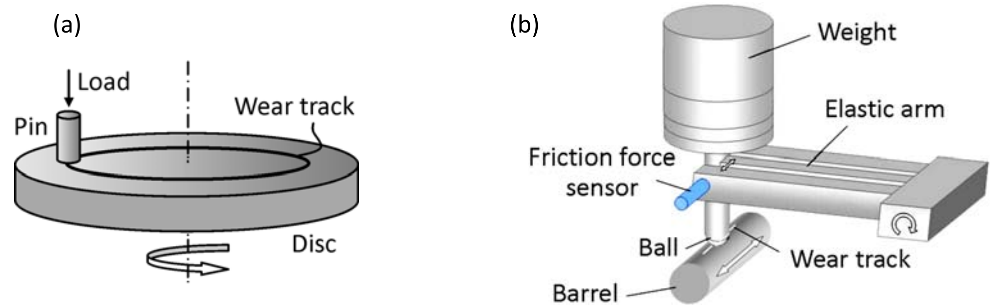

Fig. 1. Schematic drawing of the tribometer used in: (a) phase I and (b) phase II

2.2. Nanocomposites with ZnAl25Si matrix alloy (group II)

Technically pure zinc and aluminium were used to obtain the Zn25AlSi alloys (Table 2), with the addition of master alloys Al7Si and Al18Si for achieving the desired content of silicon. Strontium was added in the alloys using the master alloy Al10Sr. The alloys were melted in the laboratory electric resistance furnace. The molten alloys (570 °C) were poured in the steel moulds preheated to 200 °C. Immediately before pouring the melts were intensively manually stirred. For the purpose of comparison, a commercial ZA-27 alloy [13] was used; with the identical casting procedure as for Zn25AlSi alloys. Microstructures and mechanical properties of these materials have been presented and discussed elsewhere [4].

Table 2. Designation and properties of the tested materials (group II)

Specimen designation	Composition	Particle content, wt. %	Particle size, nm
B0	ZA-27 alloy (reference material)	–	–
B1	Zn25Al-1Si	–	–
B2	Zn25Al-1Si-0.03Sr	–	–
B3	Zn25Al-1Si-0.05Sr	–	–
B4	Zn25Al-3Si	–	–
B5	Zn25Al-3Si-0.03Sr	–	–
B6	Zn25Al-3Si-0.05Sr	–	–
B7	Zn25Al-3Si + Al_2O_3	1	20 – 30
B8	Zn25Al-3Si-0.03Sr + Al_2O_3	1	20 – 30

Nanocomposites (specimens B7 and B8 in Table 2) were produced by applying the compocasting method using Zn25Al-3Si and Zn25Al-3Si-0.03Sr as the matrix alloys, and Al_2O_3 nanoparticles as the reinforcement. The compocasting process was performed in two steps. In the first step each matrix alloy was melted, overheated at 570 °C and then cooled with 5 °C /min cooling rate to 485 °C. After that it was mixed with 50 rpm mixing rate, and continuous cooling (5 °C/min). When the melt reached temperature of 465 °C, the mixing rate was increased to 500 rpm. Mixing of the semisolid melt lasted 5 min, and then the addition of Al_2O_3 nanoparticles was then performed, that lasted 3 min. The addition of nanoparticles was carried out at a reduced mixing rate (250 rpm). After the addition of nanoparticles a short homogenization mixing (at 250 rpm) was carried out at for 3 min, and an intensive mixing (with mixing rate of 500 rpm) for 25 min. Semisolid nanocomposite mixture was poured in the steel moulds preheated at 400 °C, which is the end of the first step of the applied compocasting process. In the second step of the process a hot pressing was performed at the temperature of 350 °C and pressure of 250 MPa.

Tribological test were conducted in two phases: In the first phase (specimens B0, B1, B2, B3, B4, B5 and B6) influences of silicon and strontium addition percentage were investigated, and in the second phase (specimen B7 and B8) influences of strontium and/or Al_2O_3 nanoparticles addition were investigated. Both tests were carried out on the block-on-disc tribometer under lubricated sliding conditions, in ambient air at room temperature. Test parameters were as follows: sliding speed: 0.5 m/s; sliding distance: 1000 m; normal load: 100 N.

A schematic diagram of tribometer is presented in Fig. 2. Rectangular blocks of tested materials were used as wear test samples. Disc (counter-body) was made of steel C60E (46 to 48 HRC). Lubrication was provided by revolving of the disc which was sunk into oil container. Lubricant was mineral engine oil (SAE 15W-40, ACEA E3). Wear scars on blocks were measured in accordance with ASTM G77 with accuracy of 0.05 mm, after each test to calculate the volume loss. The values of oil temperature, coefficient of friction, normal and friction force were monitored during the test.

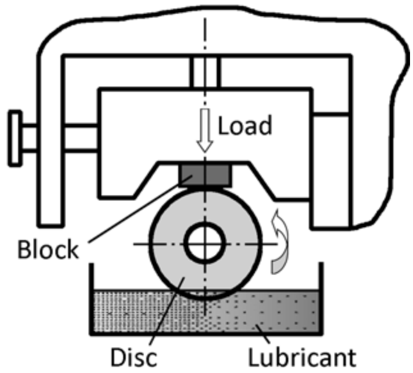

Fig. 2. Schematic drawing of the used tribometer

2.3. Micro- and nanocomposites with Cu matrix (group III)

Both Cu-based composites were produced by powder metallurgy (PM) technology, but the starting components for micro and nano Cu-based composite were different. The microcomposite was produced by PM technology (preceded by mechanical alloying) and contained micro-sized Al_2O_3 particles. Starting components were copper powder and 5 wt. % Al_2O_3 particles. This mixture was mechanically milled and compacted. The nanocomposite was produced by PM technology (preceded by mechanical alloying and internal oxidation) and contained nano-sized Al_2O_3 particles. Starting component was prealloyed copper powder containing 2.5 wt. % Al. This powder was subjected to internal oxidation, i.e. during milling aluminium, dissolved in the copper matrix, oxidizes and forms nano-sized Al_2O_3 particles (approx. 4.7 wt. %). For the purpose of comparison, a copper-based alloy Cu-0.4Cr-0.08Zr produced by casting, followed by heat treatment was used. Designation and properties of tested materials in this group are shown in Table 3. Detailed processing parameters for all materials and other properties are given elsewhere [14].

Table 3. Designation and properties of the tested materials (group III)

Specimen designation	**Composition**	**Particle content, wt. %**	**Particle size, μm**
C0	Cu-0.4Cr-0.08Zr (reference material)	–	–
C1	Cu + Al2O3	5	≈ 750
C2	Cu + Al2O3	4.7	< 100

Tribological test were conducted in two phases: In the first phase (specimens C0, C1 and C2) influences of size of reinforcement (Al_2O_3) on the macroscale (composite properties) were investigated, and in the second phase (specimen C1 and C2) the same influence were investigated on the nanoscale (only the matrix properties). Both tests were under dry sliding conditions, in ambient air at room temperature.

The phase I tests were carried out on the ball-on-disc nanotribometer (Fig. 3a) in rotation sliding mode (Fig 3b). Static body (counter-body) was a steel ball made of 100 Cr6 martensitic bearing steel with 1.5 mm in diameter. Moving body (test sample) was flat circular disc made of the tested materials. Test parameters were as follows: sliding speed: 6, 8 and 10 mm/s; normal load: 1 N; sliding distance: 30 m. Wear volumes of the test samples were calculated after each test, by measuring the wear track width, according to ASTM G99.

The values of coefficients of friction, normal and friction force, steel ball penetration depth were monitored during the test. Used nanotribometer is equipped with optical displacement sensor (fiber optic sensors) for measuring deflection of the cantilever (Fig. 3b), with high sensitivity. Light emitted from the sensor tip is reflected from the reflective areas attached to the spring, received by the sensor and converted into electrical signal. The signal is related to the distance between the sensor tip and a reflective area on the cantilever.

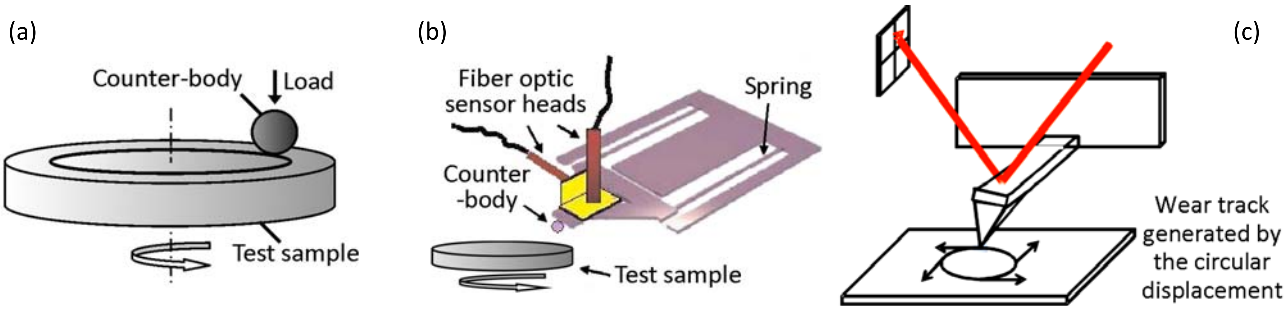

Fig. 3. Schematic drawing of the: (a) and (b) nanotribometer used in phase I (a – contact conditions; b – rotation sliding module) and (c) atomic force microscope used in phase II

The phase II tests were performed with an atomic force microscope (AFM) using the circular mode [15], schematically shown in Fig. 3c. Test parameters were as follows: normal load: 150 nN; sliding distance: ≈ 2.7 m (720.000 cycles of 1.2 μm in diameter). The coefficients of friction were also recorded.

3. RESULTS AND DISCUSSION

3.1. Microcomposites with AlSi7Mg matrix alloy (group I)

Average steady-state values of coefficients of friction, obtained in both phases of the tribological test, are shown in Table 4. All tested materials showed very similar values (0.5 to 0.7), which were in expected range for metals under dry sliding conditions (approximate values for the metals under dry sliding conditions are from 0.3 to 1.5 [17].

In the first phase of the tribological test (specimens A0, A1, A2 and A3), i.e. tests that investigated the influences of amount and size of reinforcement, the coefficient of friction values did not change significantly with the change of specific load, and one mean value per material can be accepted for the whole applied load interval. Both composite materials with 10 wt. % of Al_2O_3 (specimens A2 and A3) had higher values of the coefficient of friction than gray cast iron (specimen A0), principally due to the presence of hard reinforcing particles. Confirmation for this statement is the value of the coefficient of friction obtained with composite containing 3 wt. % of Al_2O_3 (specimen A1). In this case we have the same matrix and the same reinforcement but in lower amount, which induced lower coefficient of friction.

Table 4. The coefficient of friction average values of tested materials (group I) [11, 16]

Specimen designation	Phase I values	Phase II values
A0	0.53	–
A1	0.46	–
A2	0.61	–
A3	0.60	0.73
A4	–	0.71
A5	–	0.65

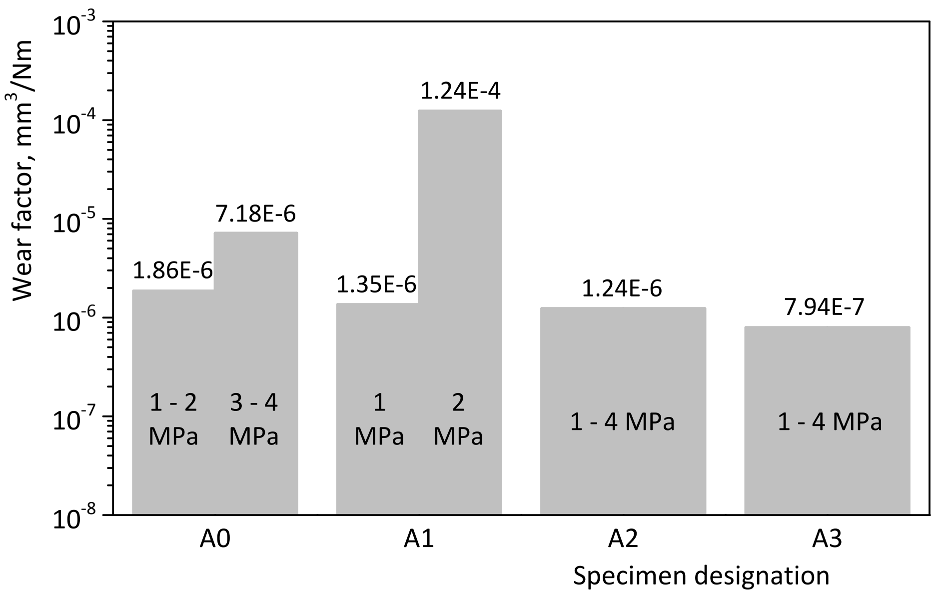

Fig. 4. Wear factors of the tested materials in the first phase (group I) [1, 16]

The wear factors, i.e. specific wear rates of the materials tested in the first phase (calculated for the steady-state period) are presented in Fig. 4. Obtained wear factor values correspond to the literature data for metallic materials in sliding contact (under unlubricated condition, and for adhesive wear, the interval is from 10^{-7} to 10^{-2} mm^3/Nm) [18]. The results show that the increase of the reinforcement amount, as well as, the increase of the reinforcement particle size had beneficial influence on the wear resistance of the composites.

For specimens A0 and A1, the existence of the critical load, at which the wear rate abruptly increases, is noted. This critical load indicates the transition of the wear regime. This transition is confirmed with the scanning electron microscopy (SEM) analysis of the worn surfaces and wear products. Gray cast iron samples (specimen A0) at lower loads (1 and 2 MPa) were not in full contact with the counter-body, and basic lamellar structure of the material could still be clearly noticed (Fig. 5a). At higher loads (3 and 4 MPa) more intensive abrasive wear starts (Fig. 5b). Adhesive wear also occurs due to the presence of high pressures and contact temperatures (Fig. 5c).

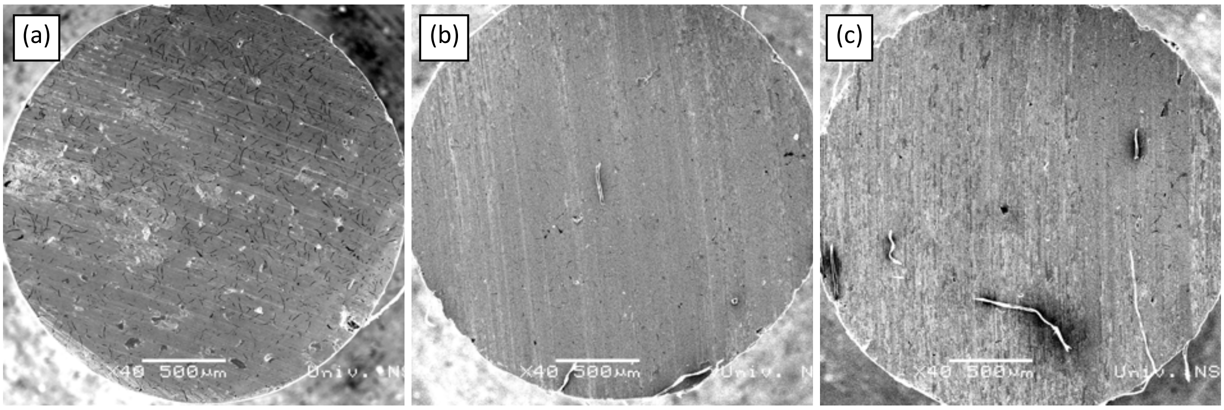

Fig. 5. SEM images of the specimen A0 (gray cast iron) pins worn surfaces, tested at different loads: (a) 2 MPa, (b) 3 MPa and (c) 4 MPa

The transition of the wear regime was especially sudden for the composite containing 3 wt. % of Al_2O_3 (specimen A1), which suggest that relatively small amount of reinforcement (3 wt. %) in this composite was enough just to support loads up to 1 MPa. At higher load (2 MPa) severe wear occur (Fig. 6a). At this load presence of the plastic flow of material on the pin surface was noticed (rounded area in Figure 6a). On the other hand, composites containing 10 wt. % of Al_2O_3 (specimens A2 and A3) at the same load did not show this plastic flow of material (Fig. 6b), and even the presence of transferred counter-body material could be noticed (rounded area in Figure 6b). Severe wear of the composite containing 3 wt. % of Al_2O_3 (specimen A1) at high load is confirmed with the SEM analysis of the wear products, i.e. in presence of the rod-like particles, longer than 50 μm were noticed (Fig. 7), which indicates existence of severe wear [19].

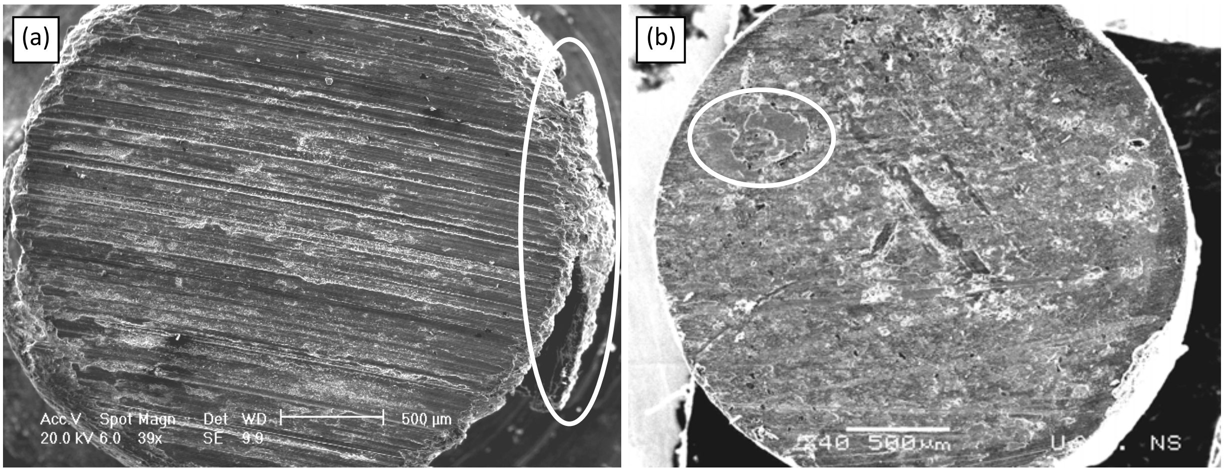

Fig. 6. SEM images of the composite pins worn surfaces at 2 MPa load: (a) specimen A1 (3 wt. % Al_2O_3) and (b) specimen A2 (10 wt. % Al_2O_3)

In the second phase of the tribological test (specimens A3, A4 and A5), i.e. tests that investigated the influences of type of reinforcement and graphite, the obtained wear factor values (Fig. 8) also correspond to the literature data for metallic materials in sliding contact. The results show that composites reinforced with SiC particles (specimens A4 and A5) have higher wear resistance, i.e. that the SiC reinforcement provided better protection of the matrix than the Al_2O_3 reinforcement, added in the same amount. The simplest explanation is the highest hardness of SiC, but we also found that the SiC particles had more favourable arrangement in the composite matrix, i.e. clusters of type B [11]. Addition of the graphite particles in composite with SiC particles (specimen A5) reduced wear rate and coefficient of friction. The presence of graphite was small (only 1 wt. %) and usually it is not enough to form the lubricant film that could effectively decrease the coefficient of friction and wear [20], so the results should be considered only as a possible trend of behaviour.

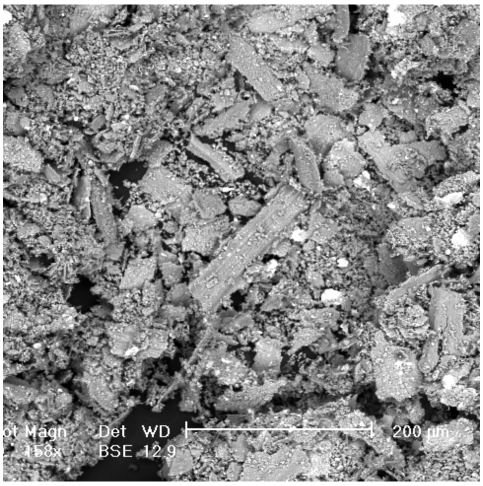

Fig. 7. SEM image of the wear products generated from specimen A1 at 2 MPa load

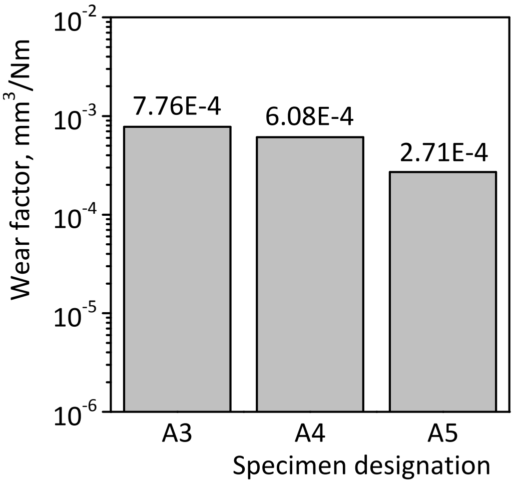

Fig. 8. Wear factors of the tested materials in the second phase (group I) [11]

SEM analysis of worn surfaces confirmed that SiC reinforcing particles were more efficient in protecting the matrix, i.e. while the presence of protruded Al_2O_3 particles on the surface was not noticed (Fig. 9a), protruded SiC particles were obvious (rounded area in Fig. 9b).

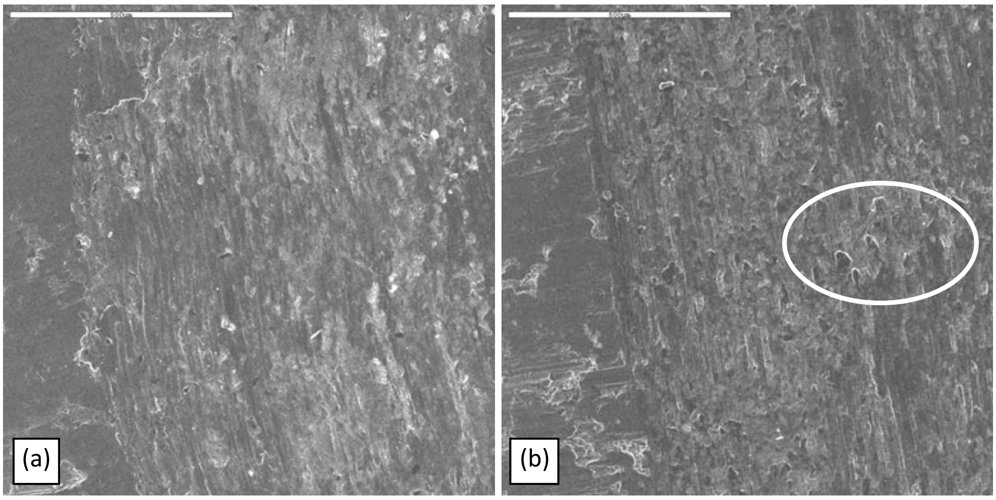

Fig. 9. SEM images of the composite samples worn surfaces: (a) specimen A3 (10 wt. % Al_2O_3) and (b) specimen A4 (10 wt. % SiC)

3.2. Nanocomposites with ZnAl25Si matrix alloy (group II)

Average steady-state values of coefficients of friction, obtained in both phases of the tribological test, are shown in Table 5. The obtained values of the coefficient of friction (0.05 to 0.1) suggest that the tests were performed in boundary lubrication regime (approximate values for the boundary lubrication are from 0.05 to 0.15 [17, 21]).

The replacement of copper with silicon (specimens B1 and B4) lowers the values of the coefficient of friction. On the other hand, addition of strontium (specimens B2, B3, B5 and B6) has negative effect on the coefficient of friction, and with increase of Sr content coefficient of friction increase further. Addition of Al_2O_3 nanoparticles (specimens B7 and B8) also increased the coefficient of friction, principally due to the higher hardness of the nanoparticles comparing to the matrix alloy. During the tests these particles were partially detached causing the three-body abrasion.

The wear factors, i.e. specific wear rates of the materials tested in the first phase are presented in Fig. 10. Wear factor values for the commercial ZA-27 alloy correspond to the literature data for the ZA-27 alloy, obtained via permanent mould casting and tested under similar conditions [22]. The results show that the size of primary silicon particles was reduced in the presence of strontium, with an improvement of their distribution in the alloy base [4, 23].

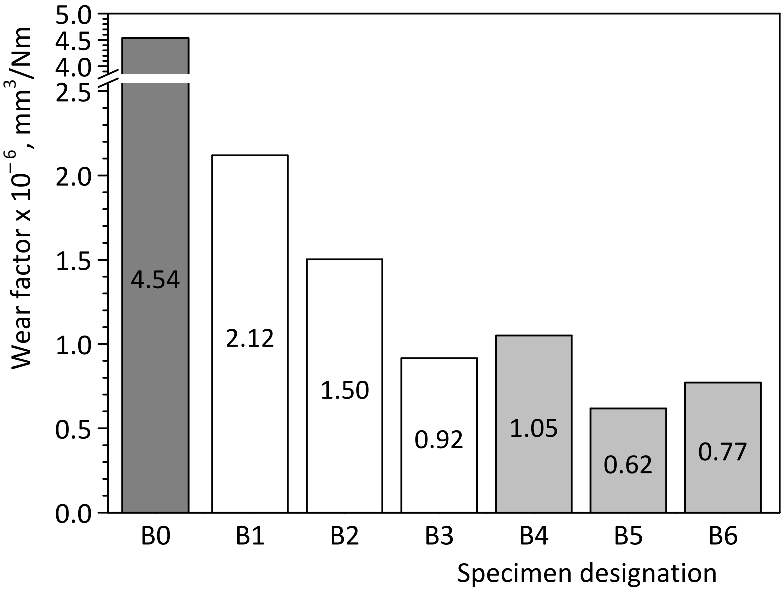

Fig. 10. Wear factors of the tested materials in the first phase (group II) [4]

Table 5. The coefficient of friction average values of tested materials (group II) [4]

Specimen designation	Phase I values	Phase II values
B0	0.069	–
B1	0.047	–
B2	0.059	–
B3	0.065	–
B4	0.061	–
B5	0.073	–
B6	0.079	–
B7	–	0.099
B8	–	0.102

SEM analysis of worn surfaces showed that the strontium modification caused the formation of independent eutectic silicon particles, which was more obvious in the alloys modified with 0.05 wt. % strontium (Fig. 11a). These particles, under the load and sliding, flow across the contact surface causing their better distribution, and thus providing better protection (Fig. 11b).

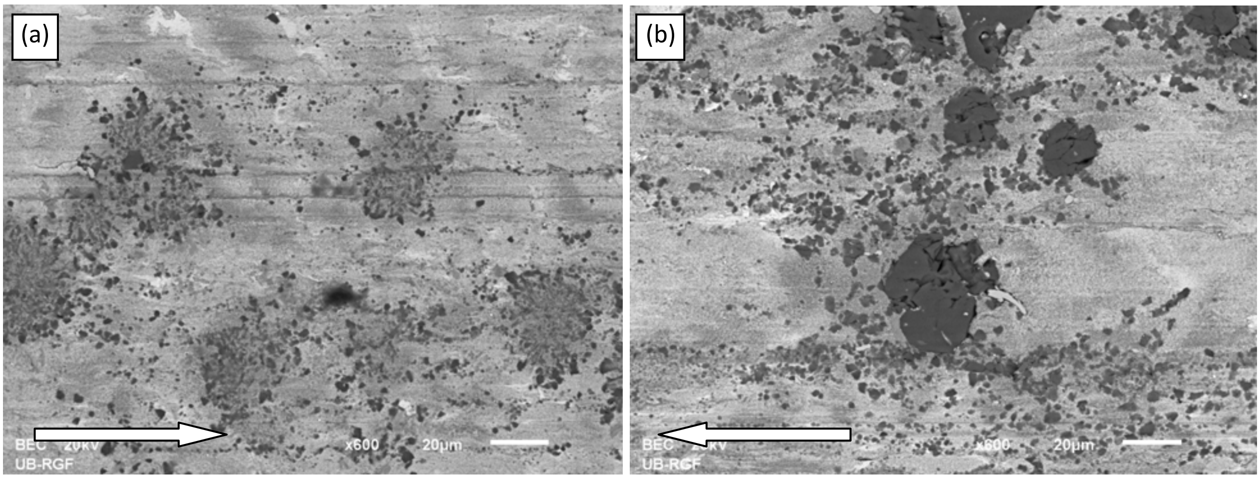

Fig. 11. SEM images of the samples worn surfaces: (a) specimen B6 (3 wt. % Si and 0.05 wt. % Sr) and (b) specimen B3 (1 wt. % Si and 0.05 wt. % Sr); counter-body sliding direction is denoted with arrows

In the case of Zn25Al-3Si alloy (specimen B4), the addition of 0.03 wt. % Sr decreased wear more than addition of 0.05 wt. % Sr, suggesting that over modification with Sr is possible situation [23]. Something similar occurred in the second phase of the tribological test (specimens B7 and B8), i.e. tests that investigated the influences of strontium and/or Al_2O_3 nanoparticles addition (which is not presented in this paper). These tests showed that the wear resistance was improved more in the case when only Al_2O_3 nanoparticles was added to the Zn25Al-3Si alloy (specimen B7) than in the case when both Al_2O_3 nanoparticles and 0.03 wt. % Sr were added to the same alloy (specimen B8).

3.3. Micro- and nanocomposites with Cu matrix (group III)

Average steady-state values of coefficients of friction, obtained in the first phase of the tribological test, are shown in Table 6. The coefficients of friction of specimens C0 (reference material) and C1 (microcomposite) were around 0.5, which is similar with the values obtained by some other researches [24], under similar sliding speed and load. Coefficient of friction of specimen C2 (nanocomposite) was more than 3 times lower in comparison with other two materials, which is connected with the fact that in this case the adhesion between sliding surfaces was less pronounced – low stick-slip phenomenon [25].

The wear factors, i.e. specific wear rates of the materials tested in the first phase (tests that investigated the influences of size of reinforcement (Al_2O_3) on the macroscale) are presented in Fig. 12. Obtained values of the wear factors are in correlation with the coefficient of friction values and correspond to the literature data for metallic materials in sliding contact [18]. The wear factor for microcomposite (specimen C1) was more than 500 times higher than for nanocomposite (specimen C2). The wt. % of Al_2O_3 particles was similar in micro- and nanocomposite (5 and 4.7 wt. %, respectively), but the size of particles was very different (≈ 750 nm and < 100 nm). It is well-known that the wear resistance increases with the decrease of the particle size for high-load, low-speed conditions (which was our case), whereas for low-load, high-speed conditions the effect is opposite [1]. Smaller particle size enabled better distribution of the nano-sized particles. Favourable distribution of nano-sized Al_2O_3 particles and its effect on slower grain growth (fine-grain structure, i.e. small grain size) reduced the deformation of matrix during sliding.

The micro-sized Al_2O_3 particles did not have the reinforcing role. On contrary, some of these particles were detached from the matrix and acts as a third body, increasing the specimen and counter-body wear. The others were protruded to the surface causing increase of the counter-body wear. For these reasons the wear of the counter-body in contact with microcomposite (specimen C1) was the highest. Detached micro-sized Al_2O_3 particles were mainly located in the worn material accumulated over the wear track (Fig. 13a). This accumulation of the worn material was not noticed at nanocomposite (specimen C2), Fig. 13b. In addition, wear of the counter-body in contact with nanocomposite was the lowest.

Table 6. The coefficient of friction average values of tested materials in the first phase (group III) [14]

Specimen designation	*v* = 6 mm/s	*v* = 8 mm/s	*v* = 10 mm/s
C0	0.43	0.48	0.46
C1	0.47	0.57	0.32
C2	0.13	0.14	0.13

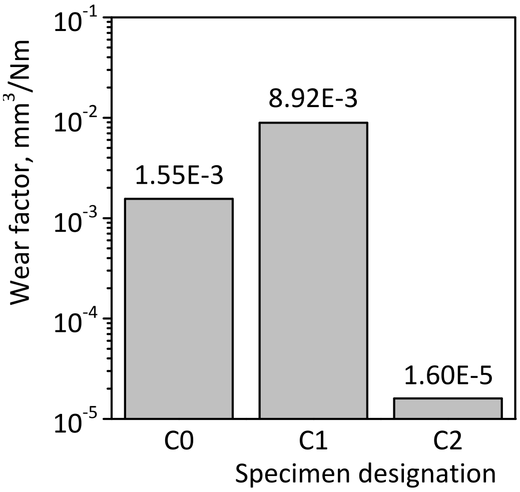

Fig. 12. Wear factors of the tested materials in the first phase (group III) [14]

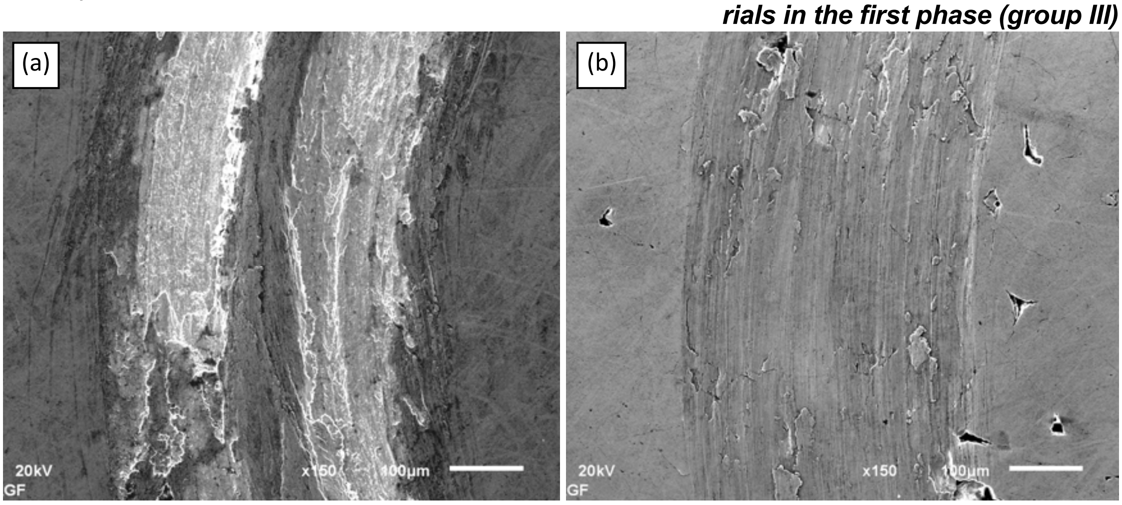

Fig. 13. SEM images of the samples worn surfaces at 8 mm/s: (a) specimen C1 (microcomposite) and (b) specimen C2 (nanocomposite); only part of the wear track is presented in both images

The tribological tests performed in the second phase (tests that investigated the influences of size of reinforcement (Al_2O_3) on the nanoscale) were just an initial one, and some more experiments is planned to completely understand composites tribological behaviour on nanoscale. In this tests only the Cu matrix is tested, since the area without Al_2O_3 particles was chose to test. The values of the coefficient of friction were similar in magnitude for the two composites (specimens C2 and C3) and showed high standard deviation. Nevertheless, the coefficient of friction for the microcomposite (specimen C2) is approximately 15 % higher. The wear rate, as measured by volume of the wear tracks, was found to be typically one order of magnitude higher for the microcomposite. This can be noticed on AFM images (Fig. 14), in which the wear tracks are clearly visible on the microcomposite sample and slightly visible on the nanocomposite sample.

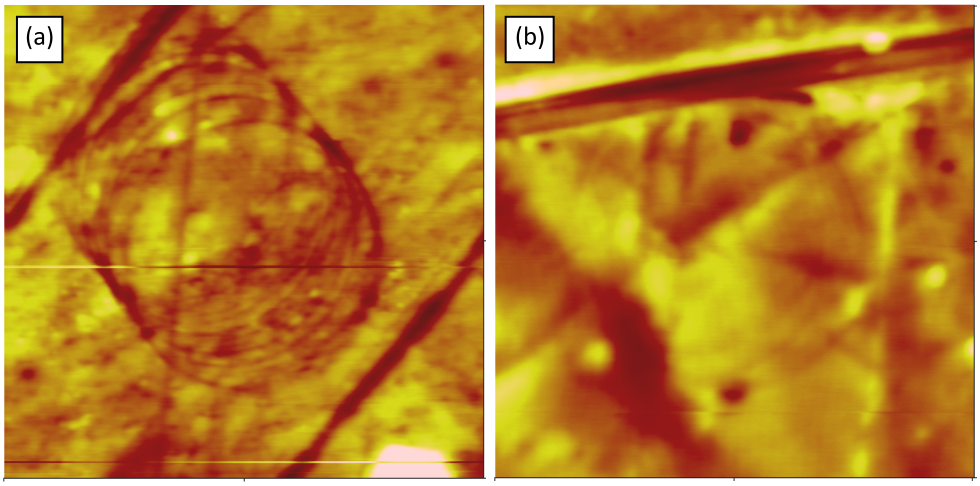

Fig. 14. AFM images (2 x 2 μm) of the samples worn surfaces: (a) specimen C1 (microcomposite) and (b) specimen C2 (nanocomposite); some shifted circular wear tracks are clearly visible on micro-composite and hardly on nanocomposite [7]

4. CONCLUSIONS

The constant development and growing application of various metal matrix composites (MMCs) is based on the fact that relatively small amount of the secondary phase (usually the reinforcing phase) can significantly improve material characteristics. The tribological properties are the most important properties that define possible application of some material in machines where parts are in contact and relative motions. Summarising the results presented in this paper it can be concluded that:

- wear of Al-Si based MMCs decreases with the increase of Al_2O_3 reinforcement amount and size;
- addition of SiC reinforcement reduces wear of Al-Si based composites more than Al_2O_3 reinforcement;
- presence of graphite in Al-Si based composites reduces the wear rate and coefficient of friction;
- replacement of copper with silicon in ZA-27 alloy, as well as, the increase of the silicon content have beneficial influence on the wear resistance;
- addition of optimal amount of strontium and/or Al_2O_3 nanoparticles to the ZnAl25Si alloy increase wear resistance;
- copper-based composites containing Al_2O_3 particles show high dependence on particle size, i.e. the nano-sized particles provide much better wear resistance than the micro-sized particles;
- modified AFM can be used for the tribological tests of small, localized areas;
- addition of the Al_2O_3 nanoparticles improves wear resistance of the Cu matrix itself.

ACKNOWLEDGMENTS

This work has been performed as a part of activities within the following projects: (a) Projects TR 34028 and TR 35021, supported by the Republic of Serbia, Ministry of Education, Science and Technological Development; (b) International Faculty Agreement of Cooperation between the Faculty of Mechanical Engineering at the University of Belgrade and the Faculty of Industrial Technology at the Technical University of Sofia; (c) CEEPUS III Network: CIIIBG0703; (d) COST Action MP1303; (e) FP7-REGPOT project 316087: AComIn (Advanced Computing for Innovation), funded by the FP7 Capacity Programme (Research Potential of Convergence Regions).

REFERENCES

1. VENCL, A., Tribology of the Al-Si alloy based MMCs and their application in automotive industry, in: Magagnin, L. (Ed.), Engineered Metal Matrix Composites: Forming Methods, Material Properties and Industrial Applications, Nova Science Publishers, New York, 2012, pp. 127-166.
2. BABIC, M., NINKOVIC, R., RAC, A., Sliding wear behavior of Zn-Al alloys in conditions of boundary lubrication, The Annals of University "Dunărea de Jos" of Galaţi, Fascicle VIII, Tribology, 2005, 60-64.
3. SAVASKAN, T., MURPHY, S., Mechanical properties and lubricated wear of Zn-25Al based alloys, Wear, 116 (2), 1987, 211-224.
4. VENCL, A., BOBIĆ, I., VUČETIĆ, F., BOBIĆ, B., RUŽIĆ, J., Structural, mechanical and tribological characterization of Zn25Al alloys with Si and Sr addition, Materials & Design, 64, 2014, 381-392.
5. MIRACLE, D.B., DONALDSON, S.L., Introduction to composites, in: ASM Handbook Volume 21, Composites, ASM International, Metals Park, 2001, pp. 3-17.
6. Glidop® Copper Dispersion Strengthened with Aluminum Oxide, SCM Metals Products, Research Triangle Park, 1994.

7. VENCL, A., MAZERAN, P.-E., NOËL, O., Friction and wear of Cu-based micro and nano composite at the macro and nanoscale, in: Proceedings of the International Conference on Understanding and Controlling Nano and Mesoscale Friction, 22-26.06.2015, Istanbul, Turkey, pp. 100.
8. VENCL, A., BOBIĆ, I., JOVANOVIĆ, M.T., BABIĆ, M., MITROVIĆ, S., Microstructural and tribological properties of A356 Al-Si alloy reinforced with Al_2O_3 particles, Tribology Letters, 32 (3), 2008, 159-170.
9. MIŠKOVIĆ, Z., BOBIĆ, I., TRIPKOVIĆ, S., RAC, A., VENCL, A., The structure and mechanical properties of an aluminium A356 alloy base composite with Al_2O_3 particle additions (MMC), Tribology in Industry, 28 (3-4), 2006, 23-27.
10. VENCL, A., BOBIĆ, I., Tribological properties of A356 Al-Si alloy base composite reinforced with Al_2O_3 particles (MMC), in: Proceedings of the 5th Congress of the Metallurgists of Macedonia, 17-20.09.2008, Ohrid, Macedonia, M8–07-E.
11. VENCL, A., BOBIC, I., AROSTEGUI, S., BOBIC, B., MARINKOVIĆ, A., BABIĆ, M., Structural, mechanical and tribological properties of A356 aluminium alloy reinforced with Al_2O_3, SiC and SiC + graphite particles, Journal of Alloys and Compounds, 506 (2), 2010, 631-639.
12. VENCL, A., BOBIC, I., STOJANOVIC, B., Tribological properties of A356 Al-Si alloy composites under dry sliding conditions, Industrial Lubrication and Tribology, 66 (1), 2014, 66-74.
13. EN 12844:1998 Zinc and zinc alloys – Castings – Specifications, 1998.
14. VENCL, A., RAJKOVIC, V., ZIVIC, F., MITROVIĆ, S., CVIJOVIĆ-ALAGIĆ, I., JOVANOVIC, M.T., The effect of processing techniques on microstructural and tribological properties of copper-based alloys, Applied Surface Science, 280, 2013, 646-654.
15. NASRALLAH, H., MAZERAN, P.-E., NOËL, O., Circular mode: A new scanning probe microscopy method for investigating surface properties at constant and continuous scanning velocities, Review of Scientific Instruments, 82 (11), 2011, 113703-1-113703-6.
16. VENCL, A., MMCs based on hypoeutectic Al-Si alloy: Tribological properties in dry sliding conditions, Tribological Journal BULTRIB, 2 (2), 2012, 17-22.
17. RAC, A., Basics of Tribology, Faculty of Mechanical Engineering, University of Belgrade, Belgrade, 1991 (in Serbian).
18. KATO, K., ADACHI, K., Wear mechanisms, in: BHUSHAN, B. (Ed.), Modern Tribology Handbook, CRC Press, Boca Raton, 2001, ch. 7.
19. VAN DRIESSCHE, M., Ferrography, Texaco Technology Ghent, Ghent, 2001.
20. YANG J.B., LIN C.B., WANG T.C., CHU H.Y., The tribological characteristics of A356.2Al alloy/$Gr_{(p)}$ composites, Wear, 257 (9-10), 2004, 941-952.
21. HAMROCK, B.J., SCHMID, S.R., JACOBSON, B.O., Fundamental of Fluid Film Lubrication, Marcel Dekker, New York, 2004.
22. RISDON, T.J., BARNHURST, R.J., MIHAICHUK, W.M., Comparative wear rate evaluation of zinc aluminum (ZA) and bronze alloys through block on ring testing and field application, SAE Technical Paper 860064, 1986.
23. JIAN, L., LAUFER, E.E., MASOUNAVE, J., Wear in Zn-Al-Si alloys, Wear, 165 (1), 1993, 51-56.
24. ZHOU, G., DING, H., ZHANG, Y., HUI, D., LIU, A., Fretting behavior of nano-Al_2O_3 reinforced copper-matrix composites prepared by coprecipitation, Metalurgija – Journal of Metallurgy MJoM, 15 (3), 2009, 169-179.
25. VENCL, A., RAJKOVIC, V., ZIVIC, F., Friction and wear properties of copper-based composites reinforced with micro- and nano-sized Al_2O_3 particles, in: Proceedings of the 8th International Conference on Tribology – BALKANTRIB '14, Sinaia, Romania, 30.10-01.11.2014, pp. 357-364.

CORRESPONDENCE

Aleksandar VENCL
University of Belgrade, Faculty of Mechanical Engineering
Kraljice Marije 16, 11120 Belgrade 35, Serbia
e-mail: avencl@mas.bg.ac.rs

Ilija BOBIĆ
Institute of Nuclear Sciences "Vinca", University of Belgrade
Mike Petrovića Alasa 12-14, 11001 Belgrade, Serbia
e-mail: ilijab@vinca.rs

Mara KANDEVA
Faculty of Industrial Engineering, Technical University – Sofia
Boulevard Kliment Ohridski 8, 1156 Sofia, Bulgaria
e-mail:; kandeva@tu-sofia.bg

Dimitar KARASTOYANOV
Institute for Information and Communication Technologies, Bulgarian Academy of Sciences
Acad. G. Bonchev St., Block 25A, 1113 Sofia, Bulgaria
e-mail: dimikara@abv.bg